



Published in final edited form as:

*Cell Mol Bioeng.* 2009 September 1; 2(3): 366–374. doi:10.1007/s12195-009-0084-4.

## Coarse-Grained Structural Modeling of Molecular Motors Using Multibody Dynamics

David Parker<sup>1</sup>, Zev Bryant<sup>2</sup>, and Scott L. Delp<sup>1,2,3</sup>

<sup>1</sup>Department of Mechanical Engineering, Stanford University, Stanford, CA 94305, USA

<sup>2</sup>Department of Bioengineering, Stanford University, Stanford, CA 94305, USA

<sup>3</sup>Schools of Medicine and Engineering Clark Center, Stanford University, Room S-321, 318 Campus Drive, Stanford, CA 94305-5444, USA

### Abstract

Experimental and computational approaches are needed to uncover the mechanisms by which molecular motors convert chemical energy into mechanical work. In this article, we describe methods and software to generate structurally realistic models of molecular motor conformations compatible with experimental data from different sources. Coarse-grained models of molecular structures are constructed by combining groups of atoms into a system of rigid bodies connected by joints. Contacts between rigid bodies enforce excluded volume constraints, and spring potentials model system elasticity. This simplified representation allows the conformations of complex molecular motors to be simulated interactively, providing a tool for hypothesis building and quantitative comparisons between models and experiments. In an example calculation, we have used the software to construct atomically detailed models of the myosin V molecular motor bound to its actin track. The software is available at [www.simtk.org](http://www.simtk.org).

### Keywords

Molecular simulation; Myosin V; Protein kinematics; Open-source software

### Introduction

Molecular motors perform central roles in fundamental biological processes, including cell division, DNA replication, muscle contraction, and intracellular transport.<sup>29</sup> Biological molecular motors are typically large protein assemblies composed of multiple polypeptide chains, with many conformational degrees of freedom. Molecular motors operate via mechanochemical cycles in which long-range conformational changes are coupled to chemical events at an enzymatic active site. Atomically detailed descriptions of the motions of molecular motors are generally not experimentally accessible, but such descriptions represent an important goal of efforts to understand the mechanisms by which molecular motors harness chemical energy to perform mechanical work.

---

Address correspondence to Scott L. Delp, Schools of Medicine and Engineering Clark Center, Stanford University, Room S-321, 318 Campus Drive, Stanford, CA 94305-5444, USA. [delp@stanford.edu](mailto:delp@stanford.edu).

Electronic Supplementary Material: The online version of this article (doi:10.1007/s12195-009-0084-4) contains supplementary material, which is available to authorized users.

## X-Ray Crystallography and Single Molecule Methods Provide Incomplete Descriptions of Molecular Motor Kinematics

Atomic structures have been determined for molecular motors crystallized in a variety of conformations and chemical states, providing important insight into the motions and mechanisms of these nanoscale machines. Crystal structures provide three-dimensional detail, but do not contain direct information about dynamics, and cannot be unambiguously assigned to functional states. Further, structures are often only available for fragments of molecular motors, since the flexibility of large protein assemblies can preclude crystallization. This challenge has been only partially addressed by fitting atomic resolution structures into low-resolution density maps obtained for larger assemblies using 3D electron microscopy<sup>45</sup> or small-angle x-ray scattering.<sup>19</sup>

Single molecule tracking and spectroscopy methods provide direct real-time information on the motions of individual molecular motors.<sup>36</sup> Translocations and conformational changes of a single protein may be tracked by attaching and visualizing an optical probe ranging in size from a single fluorophore to a micron-scale bead. Modern techniques have achieved spatial resolution on the angstrom length scale<sup>12</sup> and temporal resolution on the submillisecond timescale.<sup>42</sup> However, these measurements are typically limited to reporting on a single degree of freedom—for example, the 1D position of a motor on its track,<sup>20</sup> the angle of a probe attached to a mobile domain,<sup>10,42</sup> or the distance between a pair of fluorophores attached to specific residues in the motor.<sup>23</sup> Such measurements can constrain possible 3D models for molecular motions, but are insufficient on their own to define the kinematics of molecular motors.

## All-Atom Molecular Dynamics Simulations of Molecular Motors Are Often Impractical on Relevant Timescales

In principle, the motions of molecular motors might be directly simulated in atomic detail using molecular dynamics,<sup>37</sup> which calculates the motion of each atom in a molecular system as a point mass evolving according to Newton's equations of motion. Molecular dynamics simulations have made several interesting contributions to molecular motors research including equilibrium simulations of the myosin actin site,<sup>44</sup> steered molecular dynamics simulations of gamma rotation in the F1 ATPase,<sup>2</sup> and pulling simulations of the kinesin neck linker.<sup>16</sup> However, using molecular dynamics to simulate large systems like molecular motors is severely limited by the computational cost of calculating the nonbonded interactions between atoms in a large system and by small integration time steps, on the order of a femtosecond ( $10^{-15}$  s), required for numerical stability of a simulation. Setting aside questions of accuracy, simulation of such large systems for even a few nanoseconds requires extensive computer resources, and it is not currently feasible to carry out all-atom simulations on the millisecond timescale characteristic of molecular motor mechanochemical cycles.<sup>27</sup>

## Computational Tools Are Needed for Model Building Guided by Experiment

The goal of the work described here is to provide a computational tool that allows users to combine static, fragmentary data from crystallography with low-dimensional dynamic information from single molecule measurements, and create plausible, testable models for the structural dynamics of molecular motors. We introduce a software framework, called Protein Mechanics, that enables users to generate structurally realistic models of molecular motor conformations compatible with experimental data from different sources. The software provides an interactive environment that allows models of molecular motors to be constructed, simulated and visualized to explore protein kinematics and possible structure–function relationships. Because the software generates atomically detailed models, it can be used to predict detailed experimental results, such as differences between single molecule experiments carried out with varying probe attachment sites.

We have used Protein Mechanica to construct a coarse-grained model of myosin V, a dimeric cellular transport motor that moves hand-over-hand along an actin filament, and to examine conformations of myosin V bound to its actin track. Following Vilfan,<sup>40</sup> the simulations also allow us to calculate and compare elastic strain energies for these conformations, with implications for the mechanism of step size selection by myosin V. These calculations extend previous simple mechanical models for step size selection and processivity, and provide atomically detailed models for comparison with future experiments.

## Protein Mechanica Software

Protein Mechanica allows users to generate structurally realistic models of molecular motor conformations. To explore the large conformational changes associated with molecular motor movement, we have taken advantage of multibody dynamics methods originally developed for the simulation of macroscopic systems of interconnected rigid bodies and used for analysis of vehicle dynamics,<sup>33</sup> robotic mechanisms,<sup>28</sup> and human movement biomechanics.<sup>8</sup> Multibody dynamics methods have also been used to speed up molecular dynamics simulations while reproducing the thermodynamic properties and detailed conformational dynamics of molecular systems.<sup>4,24</sup> In contrast with other applications, the multibody dynamics employed here are not intended to directly simulate the dynamic behavior of molecular motors. Rather, they provide a convenient framework for interacting with complex articulated structures, enforcing basic physical principles such as volume exclusion, and generating hypothetical conformations whose properties may be compared with experiment.

Protein Mechanica provides an interactive environment executing on a personal computer that allows models of molecular motors to be built, visualized, and simulated without significant computational resources or substantial computer expertise. A command language allows research scientists in structural biology, biochemistry, and biophysics with no programming experience to access the functionality of the software. The command language employs terms related to the molecular structures being modeled to specify the parameters and data needed for model creation and simulation (see Supplementary materials—Appendix).

## Structural Geometry

There are few complete atomistic structures of molecular motors; thus, models of protein geometry must usually be created by combining several different atomic resolution structures. Alternatively, a model may incorporate lower-resolution electron microscopy data in the form of polygonal surfaces or substitute parametric solids, such as spheres and cylinders, for regions of a molecule. Protein Mechanica allows models to be constructed from any combination of atomistic, surface, or solid representations.

To create models of molecular structures at atomic resolution, Protein Mechanica reads files from the Protein Data Bank (PDB) that describe the atomic coordinates, atom types, and amino acid residues for a molecule structure obtained from X-ray crystallographic or NMR experiments. The fundamental structural unit in Protein Mechanica is the domain, which we define very generally in this context to mean a user-specified set of amino acid residues selected from one or more polypeptide chains (Fig. 1). Domains are the basis for substructuring a molecule for coarse-graining.

Surface representations, such as isosurfaces obtained from cryo-electron microscopy density maps, can also be used to construct molecular models. A surface is a collection of vertices and faces that define a polygonal surface or, if it is closed, a polyhedral solid. If no structural data exist for a portion of a motor assembly, then it can be represented using spheres, ellipsoids, and cylinders. These parametric solids can be created directly from molecular structures and used as simplified representations.

## Rigid Bodies

In Protein Mechanics, coarse-grained mechanical models are derived by mapping molecular domains, surfaces, and parametric solids into rigid bodies. The mass, center of mass, and moments of inertia are computed based on the geometric model. Mass properties are computed for each molecular domain using the mass and coordinates of its atoms. For a surface bounding a solid, mass properties are computed using a given density and equating the surface integrals over its closed polygon mesh with volume integrals using Gauss's Theorem.<sup>21</sup> For idealized geometry, inertial properties are computed analytically using a given density.

Rigid domains retain their atomistic representation in that the coordinates of the atoms forming the domain are translated and rotated as a rigid body during a simulation. This multiresolution representation allows a domain to interact with other domains on a fine scale while retaining its rigid nature.

## Kinematic Joints

The relative displacements and rotations between two rigid bodies are constrained by a joint. A joint is located at a common point within the bodies it connects and is constrained to remain fixed in each body as the bodies move. Different types of joints define which relative rotations are restricted between bodies. A ball joint constrains the position of a point in two bodies, but allows them to rotate freely with respect to each other. A universal joint constrains the position of a point in two bodies and allows rotation about two axes. A hinge joint constrains the position of a point in two bodies and allows rotation about a single axis.

## Modeling Physical Interactions

Protein Mechanics models two types of physical interactions: excluded volume and elasticity. The interactions that model these properties can be defined for molecular domains at multiple resolutions, from a detailed atomic level to simple geometric representations, such as spheres or ellipsoids. Interactions between domains must be explicitly defined and may be restricted to specified regions (e.g., amino acid subsets) within each domain. This approach increases computational efficiency and provides the flexibility to define interactions where they are needed.

Physical systems cannot occupy the same space at the same time. This excluded volume interaction is enforced in Protein Mechanics using a contact potential that prevents two objects from overlapping. The contact between two domain regions is checked based on the sphere or ellipsoid geometry derived from the regions assigned to the potential. If they are in contact, then forces are applied to the two regions to prevent them from penetrating (Fig. 2a).

The elasticity of a system is modeled using harmonic spring potentials defined between rigid bodies. Torsional spring potentials can be defined for each of the axes of a joint connecting two domains. An alternative is to use a spring potential connecting atoms within a given distance by a simple harmonic potential incorporating a single force constant (Fig. 2b).

Effective potentials are intended to model the collective effect of many nonbonded atomic interactions between rigid domains. Both experimental and numerical approaches can be used to parameterize effective potential energy functions for a coarsegrained representation of a molecule.

## Interactive Application of Forces to Explore Motor Conformations

In Protein Mechanics, conformations of molecular motors can be explored through the interactive application of forces specified by the user. A force can be applied to any point of a domain with a direction given by a 3D vector. Restraints can also be defined in order to align

objects during a simulation, enforcing structural conditions such as binding interactions. Restraints are implemented as harmonic springs connecting points on two domains.

The software is not intended for direct simulation of molecular motor dynamics, and does not implement either random Brownian forces or a realistic treatment of solvent viscosity. Simple damping can be specified using a damping coefficient  $B$  that produces a frictional force  $f$  and moment  $m$  for each body using

$$f = -Bv \text{ and } m = -BL\omega$$

where  $v$  and  $\omega$  are the translation and rotational velocity of a body, and  $2L$  is its characteristic length.

Simulations of coarse-grained models in Protein Mechanics are performed using computationally efficient multibody methods.<sup>31</sup> These methods solve the equations of motion used to describe the dynamic behavior of a system of rigid bodies connected by joints in linear time complexity. The result of a simulation is a time evolution of the state of each rigid body (center of mass position and orientation and their derivatives) in the coarse-grained model. The inertial dynamics we employ are inappropriate for accurately simulating molecular scale dynamics, but useful for exploring conformational space and finding accessible low-energy configurations.

## Modeling and Simulation of Myosin V

Myosin V is a two-headed motor protein that moves along actin filaments transporting cellular material within the cytoplasm.<sup>30</sup> The myosin V molecule consists of head, neck and, tail regions (Fig. 3a). The head region contains sites for actin binding and ATP hydrolysis. The neck region is a  $\sim 24$  nm long  $\alpha$ -helix extending from the head. The helix is composed of six consecutive regions, called IQ motifs, that each binds a single light chain, which can be either a calmodulin or calmodulin-like polypeptide. The stiffness of the neck is provided by the bound light chains that structurally support the flexible neck helix. The neck is followed by a coiled-coil dimerization region. The end of the tail binds to cellular cargos for transport.

Any model of myosin V should be guided by the available static structures of portions of the motor as well as by dynamic information from single molecule experiments. The catalytic head of myosin V has been crystallized in several functional states,<sup>7</sup> and additional crystal structures are available for portions of the lever arm<sup>15</sup> and the globular tail.<sup>25</sup> Electron microscopy studies of myosin V<sup>3</sup> and other myosins<sup>34</sup> bound to actin filaments provide further structural insight. A variety of single molecule tracking experiments have allowed direct real-time measurements of the displacements and rotations of different portions of the molecule,<sup>1,9,10,20,35</sup> using probes ranging from single fluorophores<sup>5,43</sup> to fluorescently labeled microtubules attached to the lever arms.<sup>32</sup> The data overwhelmingly support a model<sup>43</sup> in which the molecule “walks” hand-over-hand along the actin filament with a preferred stride size of approximately 36 nm, a distance equal to the pseudo-repeat of the actin helix. Thus, for each ATP hydrolyzed, the trailing head moves past the stationary leading head  $\sim 72$  nm to the next actin binding site, becoming the new leading head. The process continues with the two heads taking alternate steps.

A preference for  $\sim 36$  nm strides allows myosin V to walk along one face of the actin filament.<sup>20</sup> The tight step size preference has been explained using an elastic lever arm model.<sup>40</sup> It was found that if the lever arms are modeled as simple isotropic beams, the elastic strain energy will disfavor binding of the lead head to positions other than one pseudo-repeat ahead of the rear head. Elastic strain in the two-head bound state also has implications for models of processivity and chemical coordination between the two catalytic heads.<sup>18,26,38–40</sup> As an example calculation with Protein Mechanics, we sought to repeat calculations of elastic strain

energy while generating atomically detailed proposed conformations of the complete dimeric motor bound to actin.

### Coarse-Grained Model of Myosin V

All-atom models of a mouse brain myosin V monomer were constructed for amino acids 2-1080, consisting of heads in post- and pre-powerstroke states, the neck region and a portion of the coiled-coil tail region. The models were constructed using partial X-crystal structures<sup>6,11,15</sup> obtained from the Protein Data Bank and sequence similarities with other myosins.<sup>13</sup> Models of two-headed myosin V molecules were constructed by joining monomer models via their coiled-coil region (Fig. 3b).

The myosin V head-neck region was substructured into seven domains consisting of the head region and each IQ motif and its bound calmodulin (Fig. 4a). The free helix between the top of the neck and the coiled-coiled regions was substructured into four domains, and the remaining coiled-coil region was modeled as a single domain.

Rigid bodies were created from each domain and connected together using ball joints. The complete multibody system consisted of 24 rigid bodies and 22 joints, a vast simplification compared to the 35,000 atoms that make up the myosin V dimer.

Elasticity of myosin V was modeled using spring potentials between domains spanning each joint.  $C_{\alpha}$  atoms of adjacent domains within 8 Å of each other were connected with linear springs. The elastic potential used to model the stiffness of a system is given by

$$U_{ij} = \frac{1}{2} \sum C \|d_{ij} - d_{ij}^0\|^2$$

where  $d_{ij}$  is the distance between atoms  $i$  and  $j$ ,  $d_{ij}^0$  the initial distance between atoms  $i$  and  $j$ , and  $C = 35 \text{ pN nm}^{-1}$  is a uniform force constant chosen to approximately recover the bulk bending modulus ( $1500 \text{ pN nm}^2$ ) of the entire neck that was previously estimated<sup>40</sup> and supported by optical trapping measurements.<sup>22</sup>

### Simulation of Myosin V Binding to Actin

A model of the myosin V head bound to actin was created by aligning the myosin V head to a model of myosin II bound to two adjacent actin subunits,<sup>14</sup> based on electron microscopy and crystallography. This myosin V head-actin model allows the head to be positioned at a particular binding site on an actin filament. A 25 subunit actin filament was built from a seven subunit actin model<sup>17</sup> by fitting the actin model end-to-end four times.

A coarse-grained model of a myosin V dimer was created with the trailing head in a post-powerstroke state and the leading head in a pre-powerstroke state. An initial configuration of the dimer on actin was created by docking its rear head to a model of an actin filament and leaving its leading head free (Fig. 4b). Myosin V head-actin models were aligned to the actin filament 6, 9, 11, 13, 15, and 17 subunits away from the rear head to provide binding targets for the front head. Conformations of the myosin V dimer bound to these binding sites were generated by running multibody dynamics simulations using restraints between the unbound head and specific binding targets to pull the free head to a specific binding site along the actin filament. Damping was added to each rigid body to allow the system to attain a stationary state. We used damped dynamics as a means of finding low-energy conformations for each binding site, and did not intend to simulate the dynamics of the free head binding.



Visualization of the initial configuration of the myosin V leading head bound 13 subunits away from the rear head (Fig. 5) shows the dimer easily spanning the 36 nm distance between actin pseudo repeats, and generating  $3 k_B T$  of strain energy in our model. Slightly more strain energy is generated for the conformation bound 11 subunits away, whereas other conformations showed substantially higher strain energies. These results may be compared with the elastic beam model calculations of Vilfan,<sup>40</sup> and are compatible with the conclusions of Ali *et al.*, who used observations of single myosin V motors traversing suspended actin filaments to infer that the motor uses a combination of 11 subunit and 13 subunit stride sizes.<sup>1</sup> Our current model shows relatively modest increases in strain energy at very short stride sizes (not shown), which may motivate some further refinements. Examination of the elastic strain energy of specific spring potentials for conformations of a myosin V spanning different actin binding sites (Fig. 6) shows how different regions of the neck contribute to its elastic response for different stride sizes.

## Conclusion

We have developed a software framework called Protein Mechanica to construct coarse-grained models of molecular motors by substructuring them into a system of arbitrarily shaped rigid bodies connected by joints. Multibody methods incorporating interaction potentials to enforce excluded volume constraints and model system elasticity are used to generate structurally realistic models of molecular motor conformations. The multibody methodology provides a modeling tool to complement experimental and theoretical methods. Structural models generated in Protein Mechanica may be used to make detailed comparisons with single molecule tracking measurements, and calculations of elastic potentials as a function of motor conformation may later be combined with chemical kinetic models to generate detailed mechanistic models of molecular motor function.<sup>41</sup>

Protein Mechanica is currently being used to construct coarse-grained models of a two-headed myosin V attached to actin to investigate how its structure contributes to its mechanical stepping behavior. It has allowed us to propose detailed 3D conformations for myosin V bound to actin and we anticipate using the software in ongoing investigations of structure/function relationships in unconventional myosins and DNA-associated molecular motors.

## Supplementary Material

Refer to Web version on PubMed Central for supplementary material.

## Acknowledgments

This work was supported by the Stanford Bio-X Interdisciplinary Initiatives Program and by the National Institutes of Health through the NIH Roadmap for Medical Research Grant U54 GM072970 and NIH Grant DP2 OD004690. We are grateful to Russ Altman, Michael Sherman, Vijay Pande, and James Spudich for the many discussions we have had on simulation of molecular motors.

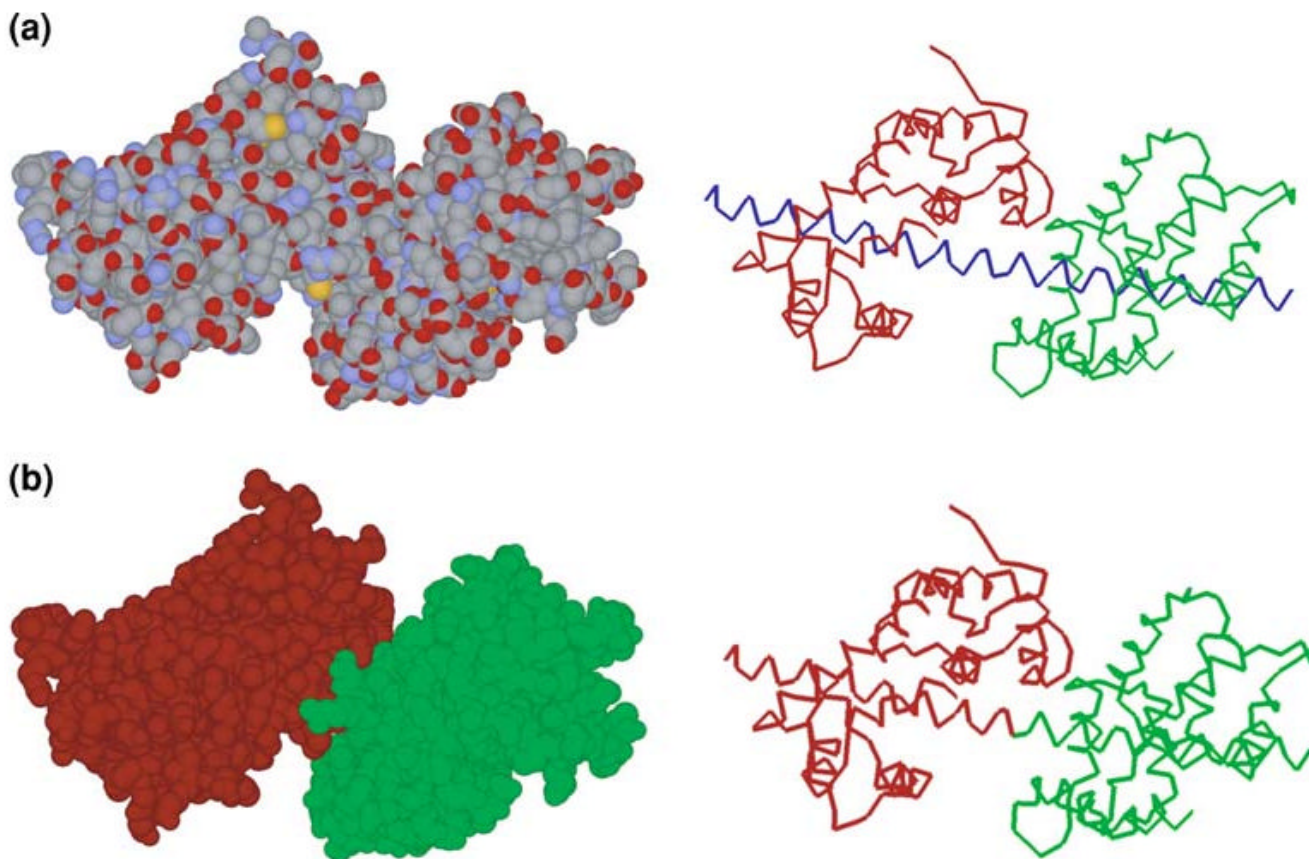
## References

1. Ali MY, et al. Myosin V is a left-handed spiral motor on the right-handed actin helix. *Nat Struct Biol* 2002;9:464–467. [PubMed: 12006986]
2. Bockmann RA, Grubmuller H. Nanoseconds molecular dynamics simulation of primary mechanical energy transfer steps in F1-ATP synthase. *Nat Struct Biol* 2002;9:198–202. [PubMed: 11836535]
3. Burgess S, et al. The prepower stroke conformation of myosin V. *J Cell Biol* 2002;159:983–991. [PubMed: 12499355]
4. Chun HM, et al. MBO(N)D: a multibody method for long-time molecular dynamics simulations. *J Comput Chem* 2000;21:159–184.

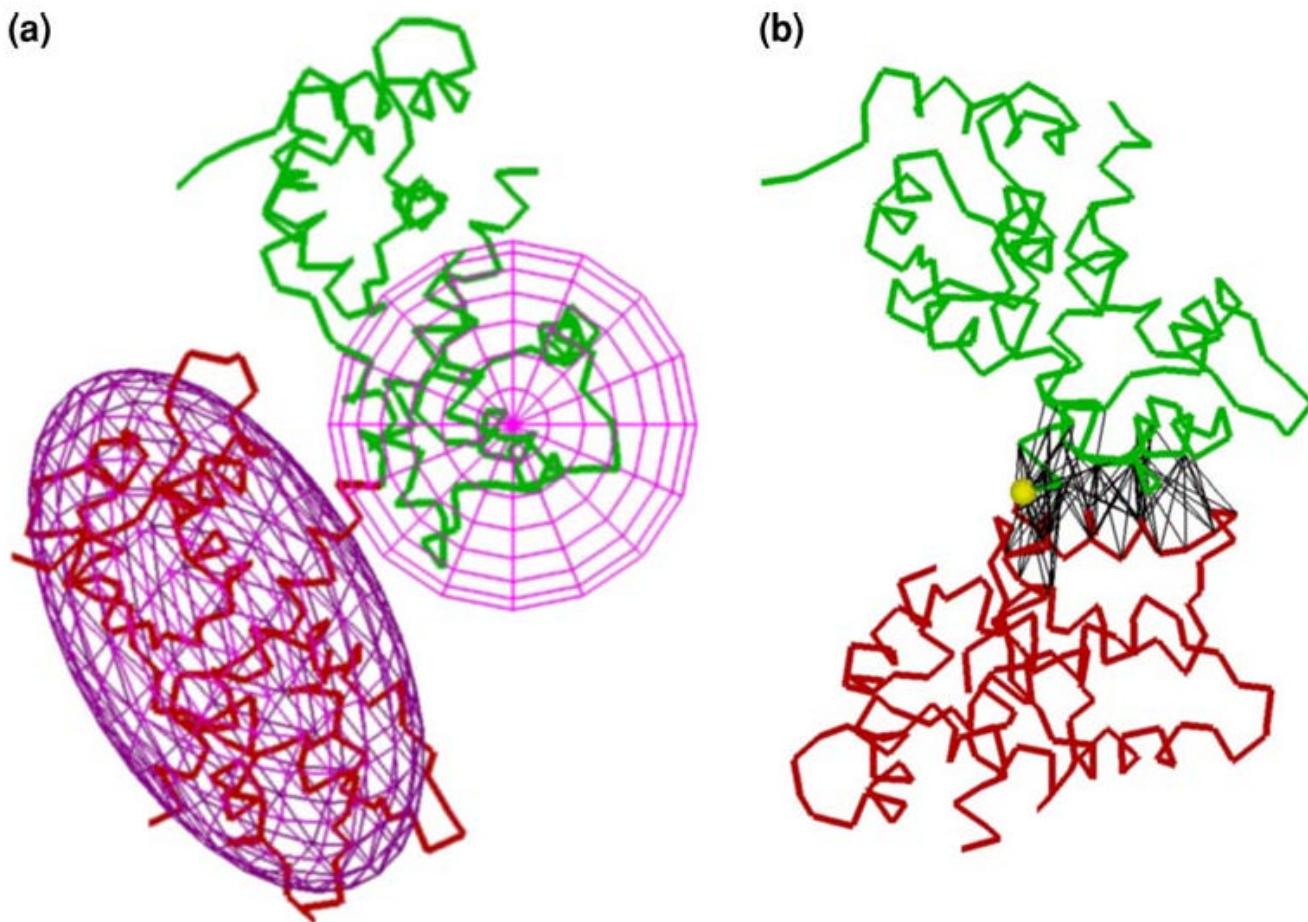
5. Churchman LS, Okten Z, Rock RS, Dawson JF, Spudich JA. Single molecule high-resolution colocalization of Cy3 and Cy5 attached to macromolecules measures intramolecular distances through time. *PNAS* 2005;102:1419–1423. [PubMed: 15668396]
6. Coureux PD, et al. A structural state of the myosin V motor without bound nucleotide. *Nature* 2003;425:419–423. [PubMed: 14508494]
7. Coureux PD, Sweeney HL, Houdusse A. Three myosin V structures delineate essential features of chemo-mechanical transduction. *EMBO J* 2004;23:4527–4537. [PubMed: 15510214]
8. De Sapio V, Khatib O, Delp S. Least action principles and their application to constrained and task-level problems in robotics and biomechanics. *Multib Syst Dyn* 2008;19:303–322.
9. Dunn AR, Spudich JA. Dynamics of the unbound head during myosin V processive translocation. *Nat Struct Biol* 2007;14:246–248.
10. Forkey JN, Quinlan ME, Alexander Shaw M, Corrie JET, Goldman YE. Three-dimensional structural dynamics of myosin V by single-molecule fluorescence polarization. *Nature* 2003;422:399–404. [PubMed: 12660775]
11. Gourinath S, et al. Crystal structure of scallop myosin S1 in the pre-power stroke state to 2.6 Å resolution: flexibility and function in the head. *Structure* 2003;11:1621–1627. [PubMed: 14656445]
12. Greenleaf WJ, Woodside MT, Block SM. High-resolution, single-molecule measurements of biomolecular motion. *Annu Rev Biophys Biomol Struct* 2007;36:171–190. [PubMed: 17328679]
13. Hodge T, Cope MJ. A myosin family tree. *J Cell Sci* 2000;113:3353–3354. [PubMed: 10984423]
14. Holmes KC, Angert I, Jon Kull F, Jahn W, Schroder RR. Electron cryo-microscopy shows how strong binding of myosin to actin releases nucleotide. *Nature* 2003;425:423–427. [PubMed: 14508495]
15. Houdusse A, et al. Crystal structure of apo-calmodulin bound to the first two IQ motifs of myosin V reveals essential recognition features. *PNAS* 2006;103:19326–19331. [PubMed: 17151196]
16. Hwang W, Lang MJ, Karplus M. Force generation in Kinesin Hinges on cover-neck bundle formation. *Structure* 2008;16:62–71. [PubMed: 18184584]
17. Kim E, et al. Cross-linking constraints on F-actin structure. *J Mol Biol* 2000;299:421–429. [PubMed: 10860749]
18. Lan G, Sun SX. Dynamics of myosin-V processivity. *Biophys J* 2005;88:999–1008. [PubMed: 15556991]
19. Lipfert J, Doniach S. Small-angle X-ray scattering from RNA, proteins, and protein complexes. *Annu Rev Biophys Biomol Struct* 2007;36:307. [PubMed: 17284163]
20. Mehta AD, et al. Myosin-V is a processive actin-based motor. *Nature* 1999;400:590–593. [PubMed: 10448864]
21. Messner AM, Taylor GQ. Algorithm 550: solid polyhedron measures. *ACM Trans Math Softw* 1980;6:121–130.
22. Moore J, Kremntsova E, Trybus K, Warshaw D. Does the myosin V neck region act as a lever? *J Muscle Res Cell Motil* 2004;25:29–35. [PubMed: 15160485]
23. Mori T, Vale RD, Tomishige M. How kinesin waits between steps. *Nature* 2007;450:750–754. [PubMed: 18004302]
24. Mukherjee RM, Crozier PS, Plimpton SJ, Anderson KS. Substructured molecular dynamics using multibody dynamics algorithms. *Int J Non Linear Mech* 2008;43:1040–1055.
25. Pashkova N, Jin Y, Ramaswamy S, Weisman LS. Structural basis for myosin V discrimination between distinct cargoes. *EMBO J* 2006;25:693–700. [PubMed: 16437158]
26. Purcell TJ, Sweeney HL, Spudich JA. A force-dependent state controls the coordination of processive myosin V. *PNAS* 2005;102:13873–13878. [PubMed: 16150709]
27. Sanbonmatsu KY, Tung CS. High performance computing in biology: multimillion atom simulations of nanoscale systems. *J Struct Biol* 2007;157:470–480. [PubMed: 17187988]
28. Schiehlen W, Guse N, Seifried R. Multibody dynamics in computational mechanics and engineering applications. *Comput Meth Appl Mech Eng* 2006;195:5509–5522.
29. Schliwa, M., editor. *Molecular Motors*. Weinheim: Wiley; 2003. p. 604
30. Sellers JR, Veigel C. Walking with myosin V. *Curr Opin Cell Biol* 2006;18:68–73. [PubMed: 16378722]



31. Shabana, AA. Dynamics of Multibody Systems. Cambridge: Cambridge University Press; 2005. p. 384
32. Shiroguchi K, Kinosita K Jr. Myosin V walks by lever action and Brownian motion. *Science* 2007;316:1208–1212. [PubMed: 17525343]
33. Sousa L, Veríssimo P, Ambrósio J. Development of generic multibody road vehicle models for crashworthiness. *Multib Syst Dyn* 2008;19:133–158.
34. Sugi H, et al. Dynamic electron microscopy of ATP-induced myosin head movement in living muscle thick filaments. *PNAS* 1997;94:4378–4382. [PubMed: 9113997]
35. Uemura S, Higuchi H, Olivares AO, De La Cruz EM, Ishiwata S. Mechanochemical coupling of two sub-steps in a single myosin V motor. *Nat Struct Biol* 2004;11:877–883.
36. Vale RD. Microscopes for fluorimeters: the era of single molecule measurements. *Cell* 2008;135:779–785. [PubMed: 19041739]
37. van der Kamp MW, Shaw KE, Woods CJ, Mulholland AJ. Biomolecular simulation and modelling: status, progress and prospects. *J R Soc Interface* 2008;5:173–190.
38. Veigel C, Wang F, Bartoo ML, Sellers JR, Molloy JE. The gated gait of the processive molecular motor, myosin V. *Nat Cell Biol* 2002;4:59–65. [PubMed: 11740494]
39. Veigel C, Schmitz S, Wang F, Sellers JR. Load-dependent kinetics of myosin-V can explain its high processivity. *Nat Cell Biol* 2005;7:861–869. [PubMed: 16100513]
40. Vilfan A. Elastic lever-arm model for myosin V. *Biophys J* 2005;88:3792–3805. [PubMed: 15792977]
41. Wang H, Oster G. Energy transduction in the F1 motor of ATP synthase. *Nature* 1998;396:279–282. [PubMed: 9834036]
42. Yasuda R, Noji H, Yoshida M, Kinosita K, Itoh H. Resolution of distinct rotational substeps by submillisecond kinetic analysis of F1-ATPase. *Nature* 2001;410:898–904. [PubMed: 11309608]
43. Yildiz A, et al. Myosin V walks hand-over-hand: single fluorophore imaging with 1.5-nm localization. *Science* 2003;300:2061–2065. [PubMed: 12791999]
44. Yu H, Ma L, Yang Y, Cui Q. Mechanochemical coupling in the myosin motor domain. I. Insights from equilibrium active-site simulations. *PLoS Comput Biol* 2007;3:e21. [PubMed: 17291159]
45. Zhou ZH. Towards atomic resolution structural determination by single-particle cryo-electron microscopy. *Curr Opin Struct Biol* 2008;18:218–228. [PubMed: 18403197]

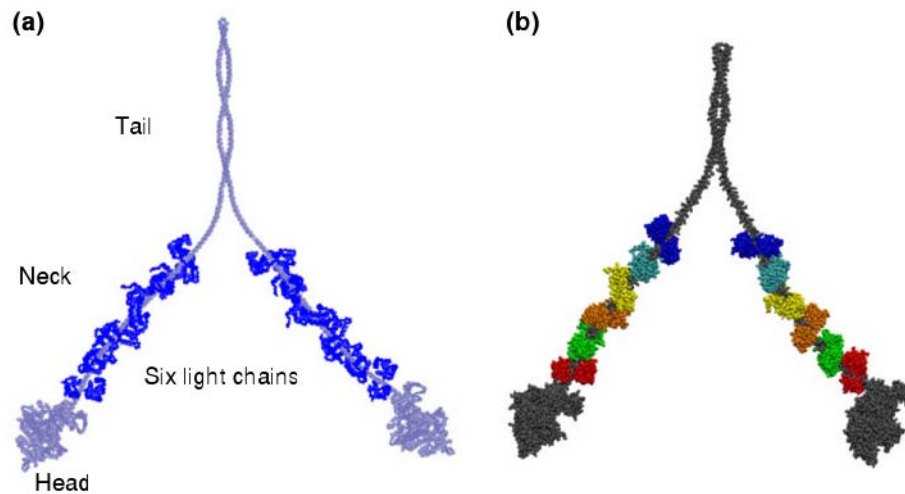


**FIGURE 1.** Domain definition and molecular representations in the Protein Mechanica software. (a) Visualization of the atomic structure of two calmodulin molecules bound to the central  $\alpha$ -helix. In the space-filling representation (*left*), atoms are colored by atom type. In the  $C_{\alpha}$  backbone trace representation (*right*), the calmodulin chains are colored red and green, and the helix is blue. (b) Two domains (*colored red and green*) defined to each comprise a portion of the  $\alpha$ -helix together with its bound calmodulin. The domains are shown using space-filling atoms (*left*) and  $C_{\alpha}$  backbone (*right*) representations.

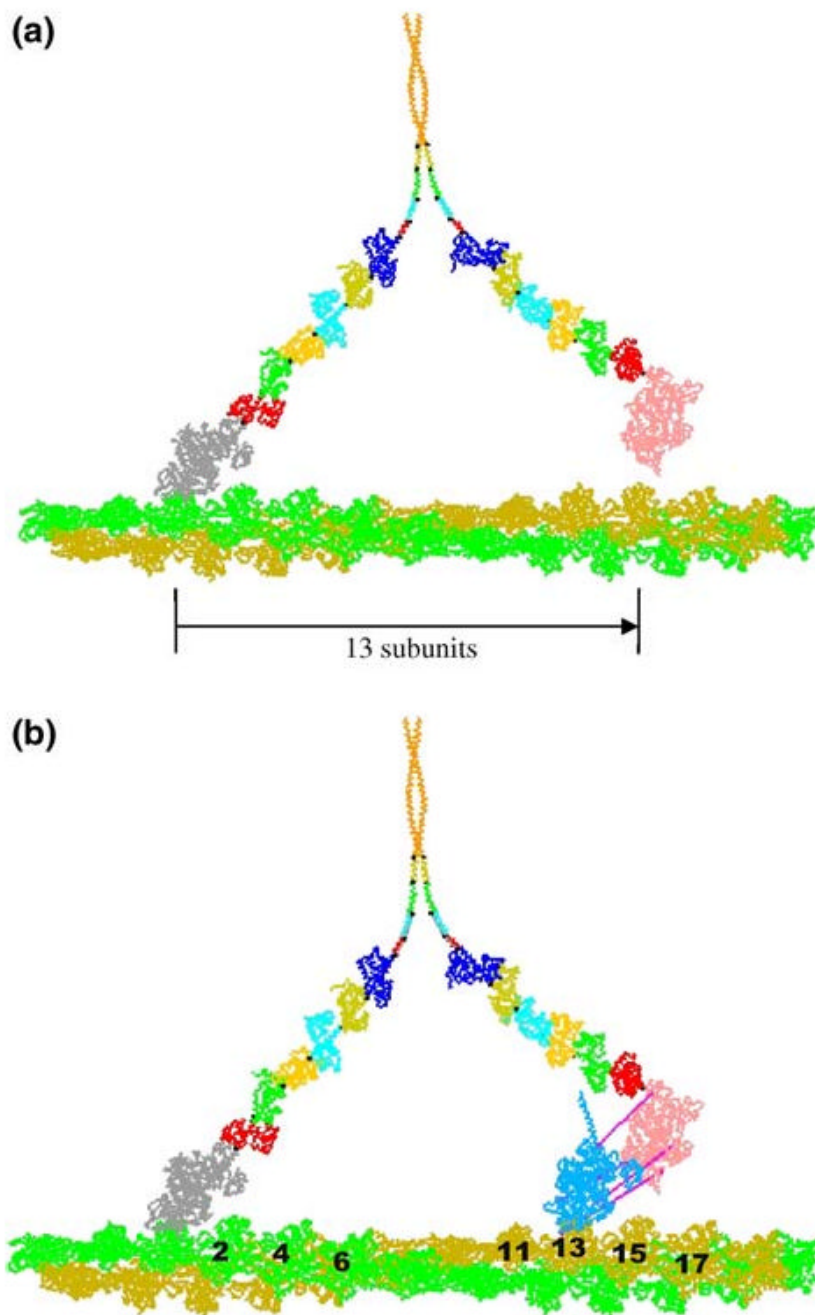


**FIGURE 2.**

Modeling physical interactions. (a) Contact potential geometry for two rigid domains (*colored red and green*), each comprising a calmodulin molecule bound to a myosin V IQ motif helix (*colored red and green*). An ellipsoid has been defined for the entire lower domain while a sphere has been defined for a portion of the upper domain (*colored purple*). (b) A spring potential defined for two rigid domains.  $C_{\alpha}$  atoms between the two domains within 8 Å of each other are connected by harmonic springs shown as *black lines*.



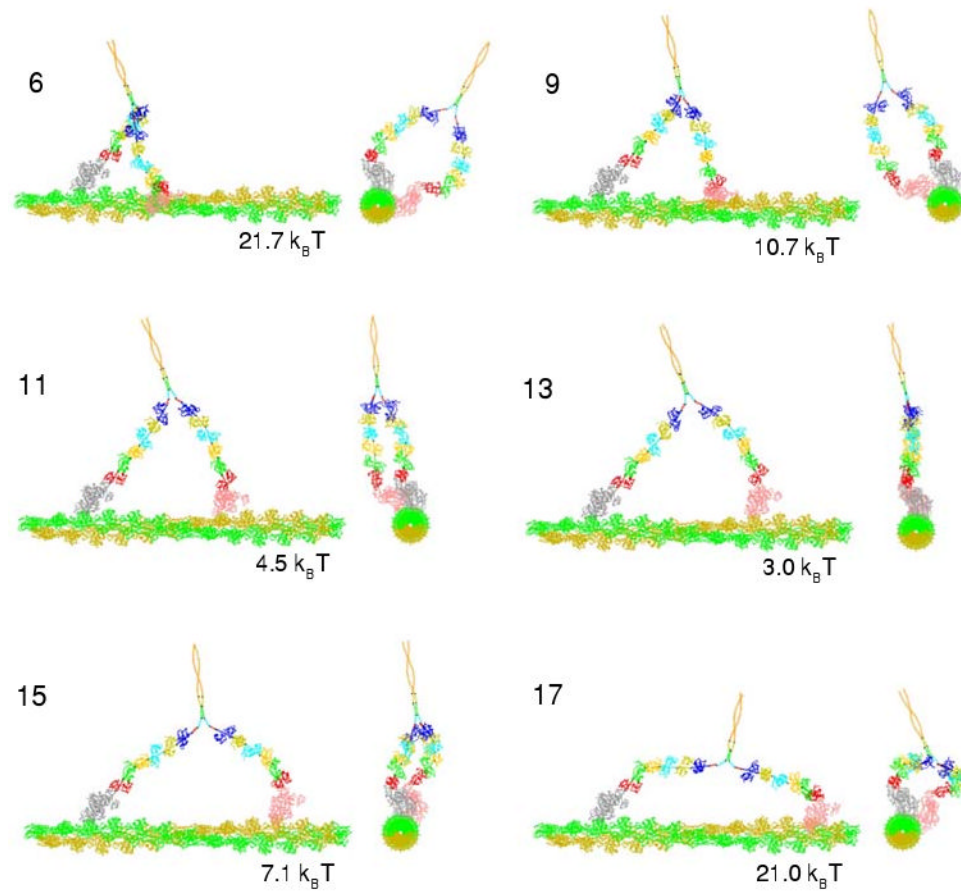
**FIGURE 3.** Structure and coarse-grained model of the myosin V molecule. (a) A myosin V molecule (*gray*) consists of head, neck, and tail regions. The head region binds actin and hydrolyzes ATP. Extending from the head is the neck region, a long  $\alpha$ -helix containing six IQ motifs, each of which binds a single calmodulin-like light chain (*blue*). The  $\alpha$ -helices of two myosin V molecules dimerize to form a coiled-coil tail region. (b) Atomic resolution model of the myosin V dimer.



**FIGURE 4.**

Coarse-grained model of a myosin V dimer. (a) Each myosin monomer has been substructured into 12 rigid bodies (shown using a  $C_{\alpha}$  backbone representation and different colors for each domain) connected by ball joints (shown as *black spheres*). The rear and leading heads are in a post-powerstroke and pre-powerstroke conformation, respectively. The rear head (*colored gray*) is bound to an actin filament (*colored green and yellow*) while the leading head (*colored pink*) is free. (b) Restraints (*colored purple*) defined between the free head and a “ghost” actin-bound reference head (*colored blue*) will pull the free head and align it to the desired binding site during a simulation. Actin subunits are numbered on the actin filament relative to the binding site of the trailing head.



**FIGURE 5.**

Conformations of a myosin V dimer spanning different numbers of actin binding sites. The leading head (*colored pink*) is bound 6, 9, 11, 13, 15, or 17 actin subunits from the bound rear head (*colored gray*). The elastic strain energy for each conformation is shown below the actin filament.



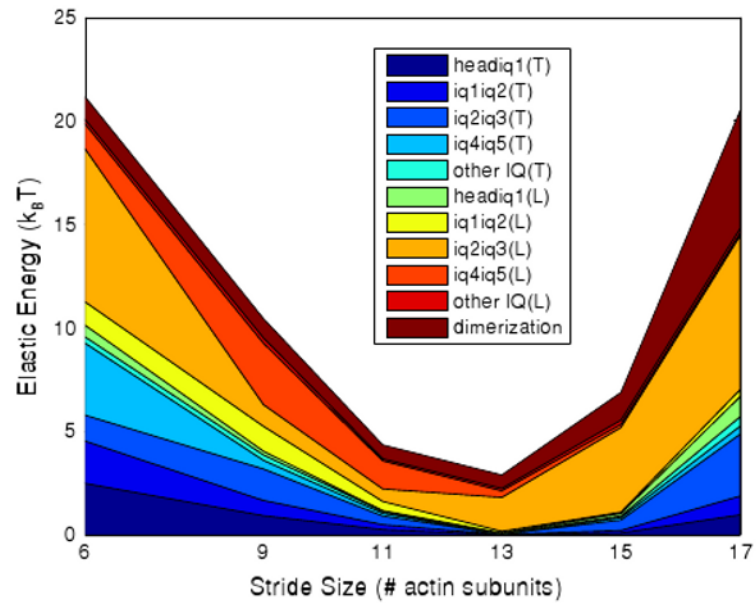


**FIGURE 6.** Distribution of elastic strain energy for conformations of a myosin V dimer spanning different numbers of actin binding sites. An area chart breaks down the energetic contributions of strain localized to joints between numbered IQ domains in the leading (L) and trailing (T) myosin neck regions, as well the contribution of strain at the dimerization region for our model of myosin V.